Spin Selectivity in Electron Transmission Through Self-Assembled Monolayers of Double-Stranded DNA

B. Göhler, *et al.*

Science **331**, 894 (2011);
DOI: 10.1126/science.1199339

tion pattern for $P_0 = 2$ bar recorded at a mass of 8 amu is shown in Fig. 2C. In this measurement, additional peaks are present, and their positions agree nicely with the calculated diffraction angles of the helium trimer. These findings are fully consistent with previous observations that more trimers are formed at increased stagnation pressure (*12*). In addition, it is known that trimers are more efficiently detected at a mass of 8 amu than dimers (*11*), further enhancing the trimer peaks relative to those of the dimer.

The observed nondestructive scattering of He_2 as well as He_3 from a reflection grating exemplifies the peculiar nature of a quantum-mechanical impact. Quantum reflection causes helium dimers and trimers to reflect tens of nanometers above the actual surface, where surface-induced forces are too feeble to break up even the fragile He_2 bond.

References and Notes

1. H. Friedrich, G. Jacoby, C. G. Meister, *Phys. Rev. A* **65**, 032902 (2002).
2. F. Shimizu, *Phys. Rev. Lett.* **86**, 987 (2001).
3. H. Oberst, Y. Tashiro, K. Shimizu, F. Shimizu, *Phys. Rev. A* **71**, 052901 (2005).
4. V. Druzhinina, M. DeKieviet, *Phys. Rev. Lett.* **91**, 193202 (2003).
5. B. S. Zhao, S. Schulz, S. Meek, G. Meijer, W. Schöllkopf, *Phys. Rev. A* **78**, 010902 (2008).
6. F. Luo, G. C. McBane, G. Kim, C. F. Giese, W. R. Gentry, *J. Chem. Phys.* **98**, 3564 (1993).
7. W. Schöllkopf, J. P. Toennies, *Science* **266**, 1345 (1994).
8. R. E. Grisenti *et al.*, *Phys. Rev. Lett.* **85**, 2284 (2000).
9. F. Knauer, O. Stern, *Z. Phys.* **53**, 779 (1929).
10. I. Estermann, O. Stern, *Z. Phys.* **61**, 95 (1930).
11. W. Schöllkopf, J. P. Toennies, *J. Chem. Phys.* **104**, 1155 (1996).
12. L. W. Bruch, W. Schöllkopf, J. P. Toennies, *J. Chem. Phys.* **117**, 1544 (2002).
13. K. T. Tang, J. P. Toennies, C. L. Yiu, *Phys. Rev. Lett.* **74**, 1546 (1995).

14. We thank J. R. Manson for insightful discussions. B.S.Z. acknowledges support by the Alexander von Humboldt Foundation and by the Korea Research Foundation Grant funded by the Korean Government (KRF-2005-214-C00188).

25 November 2010; accepted 12 January 2011
10.1126/science.1200911

Spin Selectivity in Electron Transmission Through Self-Assembled Monolayers of Double-Stranded DNA

B. Göhler,[1] V. Hamelbeck,[1] T. Z. Markus,[2] M. Kettner,[1] G. F. Hanne,[1] Z. Vager,[3] R. Naaman,[2]* H. Zacharias[1]

In electron-transfer processes, spin effects normally are seen either in magnetic materials or in systems containing heavy atoms that facilitate spin-orbit coupling. We report spin-selective transmission of electrons through self-assembled monolayers of double-stranded DNA on gold. By directly measuring the spin of the transmitted electrons with a Mott polarimeter, we found spin polarizations exceeding 60% at room temperature. The spin-polarized photoelectrons were observed even when the photoelectrons were generated with unpolarized light. The observed spin selectivity at room temperature was extremely high as compared with other known spin filters. The spin filtration efficiency depended on the length of the DNA in the monolayer and its organization.

Double-stranded DNA (dsDNA) is chiral both because of its primary structure and because of its secondary, double helix, structure. Owing to its broken mirror image symmetry, when a charge moves within a chiral system in one direction, it creates a magnetic field. The direction of spin polarization of photoelectrons emitted from nonmagnetic substrates, which exhibit high spin-orbit coupling, depends on the handedness of the circularly polarized light. Photoelectrons emitted from a bare gold substrate upon exposure to linearly polarized light would not be expected to show spin polarization. An organic chiral layer on a nonmagnetic metal surface is not expected to be self-magnetized, and photoelectrons ejected from such a layer with linearly polarized light would also be unpolarized. However, we observed exceptionally high polarization of electrons ejected from surfaces coated with a self-assembled monolayer of dsDNA, independent of the polarization of the incident light. By directly measuring the spin of the transmitted electrons with a Mott polarimeter, we found spin polarizations exceeding 60% at room temperature. This observation establishes the prospect of using dsDNA, or other chiral molecules, as a spin filter.

Unconventional magnetic properties affecting spin transport have been reported for inorganic-inorganic interfaces (*1*), topological insulators (*2*), graphene (*3*, *4*), and organic molecules adsorbed on magnetic substrates (*5*). Organic molecules would seem unlikely candidates for spin-selective transport properties because of their weak spin-orbit coupling. However, studies of photoelectrons ejected from gold surfaces covered with self-assembled, organized monolayers of chiral molecules show that the emission intensity depends on the circular polarization of the exciting light (*6*) as well as the voltage across the layer and its handedness (*7*, *8*). In these studies, the spin of the transmitted electron was not measured directly, and spin-dependent transmission was inferred from the dependence of the total electron transmission on the circular polarization of the incident photons. Furthermore, those studies could not directly determine whether the ejected electrons are highly polarized when the incident photons are unpolarized, or if the effect results simply from circular dichroism, namely, that the absorption of the system depends on the light circular polarization (*9*).

[1]Physikalisches Institut, Westfälische Wilhelms-Universität Münster, D-48149 Münster, Germany. [2]Department of Chemical Physics, Weizmann Institute, Rehovot 76100, Israel. [3]Department of Particle Physics and Astrophysics, Weizmann Institute, Rehovot 76100, Israel.

*To whom correspondence should be addressed. E-mail: ron.naaman@weizmann.ac.il

The sample preparation is similar to that described in (*10*). Self-assembled dsDNA monolayers are prepared according to standard procedures by depositing dsDNA, which is thiolated on the 3′ end of one of the DNA strands [see Supporting Online Material (*10*)] on a clean gold substrate (*11*) (Fig. 1). Four different lengths of dsDNA were investigated: 26, 40, 50, and 78 base pairs (bp) long. We used either polycrystalline Au or single-crystal Au(111) as substrates. The monolayers were characterized by various methods that ensure the uniformity and reproducibility of the DNA layer (*12*). The experiments were carried out under ultrahigh-vacuum conditions. Two photoelectron detection schemes were used: an electron time-of-flight instrument that recorded the kinetic energy distribution of the electrons and a Mott-type electron polarimeter for spin analysis (figs. S1 to S3). The photoelectrons were ejected by an ultraviolet (UV) laser pulse with photon energy of 5.84 eV, pulse duration of about 200 ps at 20-kHz repetition rate, and a fluence of 150 pJ/cm^2. The laser light was incident normal to the sample and was either linearly or circularly polarized. No damage was observed during the course of the spin polarization measurement (~4 hours).

For direct polarization measurements, the photoelectrons were guided by an electrostatic 90°-bender and subsequent transport optics. Hence, an initial longitudinal spin polarization is converted into a transverse one for analysis. In the electron polarimeter, an electron spin polarization causes a scattering asymmetry $A = (I_U - I_L)/(I_U + I_L)$. Here $I_{U,L}$ denotes the count rates in the upper and lower counter in the Mott polarimeter (fig. S1) (*13*, *14*). The transverse polarization is given by $P = A/S_{eff}$. The analyzing power, the Sherman function (*15*), was calibrated to be $S_{eff} = -(0.229 \pm 0.011)$ (fig. S4). We measured the spin polarization parallel to the sample normal and thus parallel to the initial electron velocity.

The spin polarization of photoelectrons from a clean Au(111) single crystal and the sign of its orientation depend on the laser polarization (Fig. 2A). An intensity asymmetry of $A = (5.03 \pm 1.1)\%$ was observed. Combined with the Sherman function S_{eff}, an electron spin polarization of $P = -(22 \pm 5)\%$ was determined for emission from

the single-crystal substrate. As expected, when the laser was polarized linearly, no spin polarization was observed. For reference, the spin polarization for electrons emitted from the molybdenum sample holder was zero for circular as well as linear laser polarization (fig. S5).

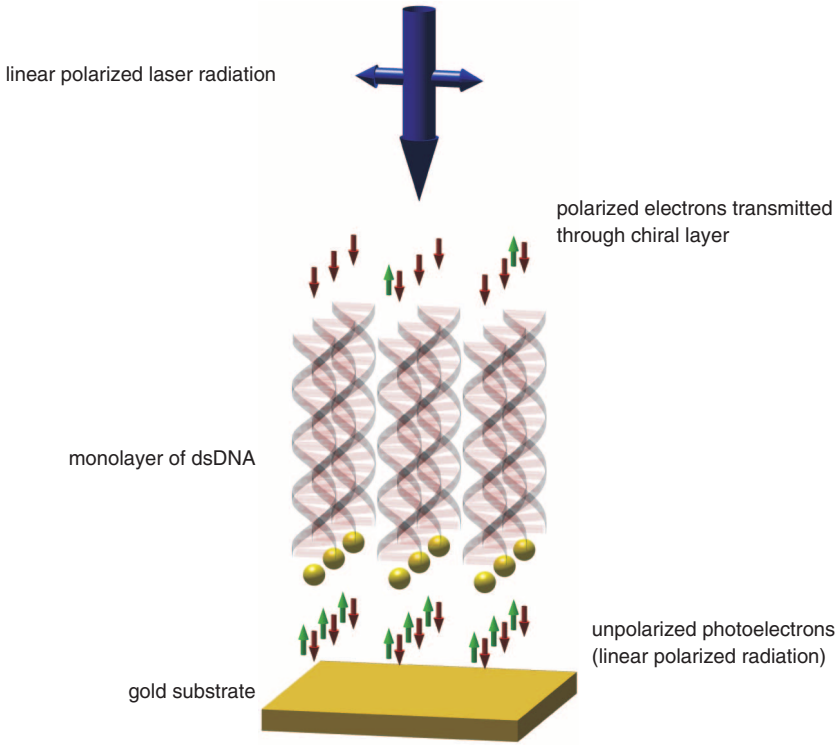

Fig. 1. A scheme describing the monolayer of dsDNA as spin filter. Unpolarized electrons are ejected from the gold substrate by a linearly polarized light. Most of the electrons transmitted through the DNA are polarized with their spin aligned antiparallel to their velocity. The electrons that are not transmitted are captured by the DNA and tunnel back to the grounded substrate within the time period between two laser pulses.

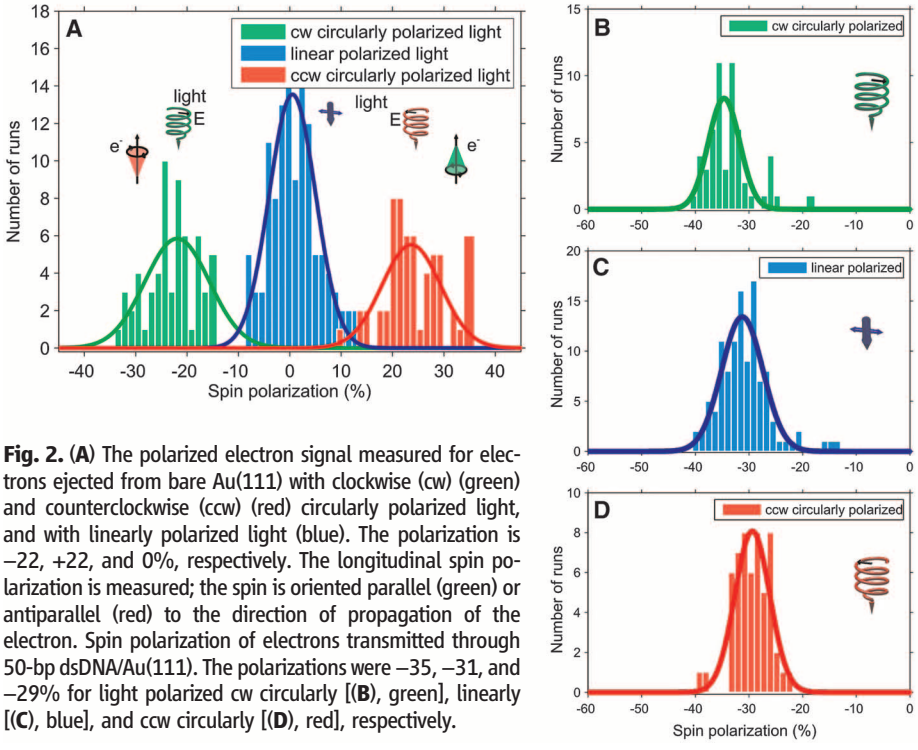

Fig. 2. (**A**) The polarized electron signal measured for electrons ejected from bare Au(111) with clockwise (cw) (green) and counterclockwise (ccw) (red) circularly polarized light, and with linearly polarized light (blue). The polarization is −22, +22, and 0%, respectively. The longitudinal spin polarization is measured; the spin is oriented parallel (green) or antiparallel (red) to the direction of propagation of the electron. Spin polarization of electrons transmitted through 50-bp dsDNA/Au(111). The polarizations were −35, −31, and −29% for light polarized cw circularly [(**B**), green], linearly [(**C**), blue], and ccw circularly [(**D**), red], respectively.

The spin polarization of electrons from the same Au(111) single crystal, transmitted through a self-assembled monolayer of 50-bp dsDNA, was measured for excitation with clockwise (cw) (Fig. 2B) and counterclockwise (ccw) (Fig. 2D) circularly polarized light, and linearly (Fig. 2C) polarized light. Strongly spin-polarized electrons with average polarizations of −(35 ± 3)%, −(29 ± 3)%, and −(31 ± 4)%, respectively, were observed, and all the spin polarizations showed the same negative sign, independent of the light polarization. The ordered monolayer of dsDNA acts as a spin filter for photoelectrons emitted from the gold surface.

A systematic study of the dependence of the degree of electron spin polarization on the length of the dsDNA was carried out on polycrystalline gold substrates (fig. S7). For a bare polycrystralline gold substrate, a spin polarization of essentially zero is observed (fig. S8). When a polycrystalline substrate was coated with a self-assembled monolayer of dsDNA, a strong spin polarization was observed. The spin polarization observed for electrons transmitted through a monolayer of 78-bp DNA is shown for cw (Fig. 3A) and ccw (Fig. 3C) circularly polarized light, and for linearly (Fig. 3B) polarized light. The average polarizations are $P = -(55 \pm 7)\%$, $-(61 \pm 6)\%$, and $-(57 \pm 6)\%$, respectively, again nearly independent of the light polarization. The observed spin polarization of −61% translates into

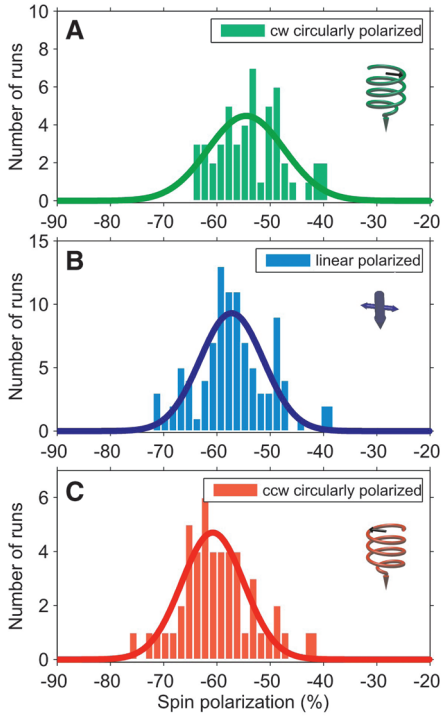

Fig. 3. The photoelectron polarization as measured for electrons ejected from a poly(Au)-coated substrate with a monolayer of 78-bp dsDNA. For the cw circularly polarized light, the electron polarization is −(54.5 ± 7.0)% [(**A**), green]; for the linearly polarized light, the polarization is −(57.2 ± 5.9)% [(**B**), blue]; and for the ccw polarized laser, the electron polarization is −(60.8 ± 5.8)% [(**C**), red].

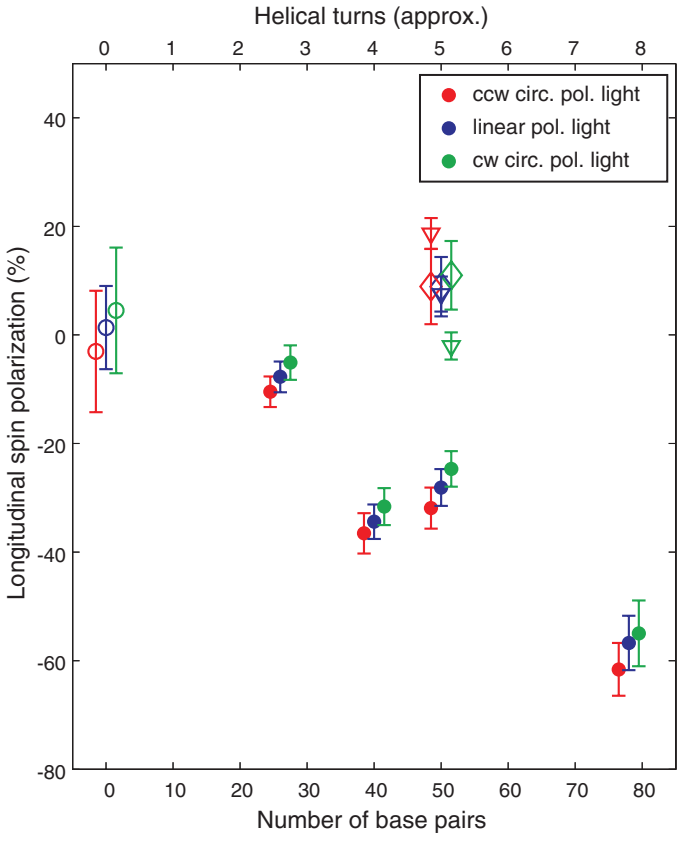

Fig. 4. The electron spin polarization for various monolayers of DNA, consisting of different numbers of double-stranded base pairs (filled circles), monolayers of ssDNA (open diamonds), sample of dsDNA damaged by UV light (open triangles), and uncleaned bare polycrystalline gold substrate (open circles). Measurements were conducted with cw, ccw, and linearly polarized light (green, red, and blue, respectively). For clarity, the symbols for the different light polarizations are offset by plus and minus 1 bp. Whereas for the dsDNA, on average, the polarization increases with the length of the DNA, no polarization is obtained for the ssDNA. For the dsDNA, the polarization increases slightly when the electrons are injected with ccw circularly polarized light, because the electrons injected into the layer are spin polarized with polarization that coincides with the spin selectivity of the monolayer. The error bars represent the SD resulting from variation between the different monolayers measured.

a ratio of 4.1:1 for left- to right-handed spins in the transmitted electron flux. In Fig. 4, the electron spin polarization is presented for four different monolayers of dsDNA of different lengths. The results of 40 different experiments on 12 different samples are shown. Increasing the length of the dsDNA tends to increase the absolute value of electron spin polarization. Also shown in Fig. 4 are polarization results when the sample was damaged by UV radiation and when the gold was coated by a monolayer of single-stranded DNA. In these latter cases, no net spin selectivity could be observed.

The results presented here indicate that well-organized self-assembled monolayers of dsDNA on Au act as very efficient spin filters. The spin selectivity depends on the organization of the molecules, and within the range of DNA length studied, the selectivity increases with its length. Even the longest molecules that we used are still shorter than the persistence length of the DNA, which is the minimal length where notable changes from rigid rods are observed. Hence, the DNA oligomers studied here are rigid and the monolayer can be visualized as consisting of rigid chiral rods closely packed together (Fig. 1). In the case of a monolayer made from single-stranded DNA (ssDNA), the molecules are more floppy and do not form rigid close-packed monolayers (*8*), and indeed no spin selectivity is observed. Because the photon energy is lower than the ionization energy of the DNA and the laser intensity is low, the photoelectrons all originate from the gold substrate. In addition, less than 0.1% of the incident light is absorbed in the layer, even under resonance conditions. The low intensities and weak absorbance ensure further that nonlinear excitation processes do not occur in the DNA layer.

Several groups have reported on experiments in which electrons were transmitted through free-standing (*16*, *17*) or supported (*18*–*21*) thin ferromagnetic films that acted as a spin filter. In these cases and for low-energy electrons, the selectivity was about 25% (*17*). In these experiments, the spin polarization can be explained by inelastic electron scattering involving unoccupied d states above the Fermi level. The scattering rate for minority spin electrons is then enhanced with respect to that of majority spin electrons because of an excess of minority spin holes (*22*, *23*). In those experiments, the polarization decreased sharply as a function of collision energies, owing to the spin dilution by secondary electrons (*20*). In the present work, the polarization is energy independent within the energy range (E_{kin} = 0 to 1.2 eV) studied. Although no extensive optimization has been performed and polarized light is not needed, the polarization achieved in the present system is almost as high as that obtained by photoemission with circularly polarized light from artificially strained GaAs substrate (70 to 80%) (*24*).

The mechanism of how charge transport or charge redistribution through chiral systems generates a magnetic field is elementary; however, this magnetism is transient and ends when the charge flow stops. A possible way to transform transient charge flow into permanent magnetism is by spin-orbit coupling that converts the angular momenta of the electrons into spin alignment. Spin-orbit coupling in hydrocarbons is commonly believed to be very weak, and no appreciable spin alignment is expected. Indeed, the interaction of spin-polarized electrons with chiral molecules has been studied (*25*). When these electrons were scattered from the gas phase and thus randomly oriented chiral molecules, only a very small preference on the order of 10^{-4} of one spin orientation over the other was found, and only when a heavy metal atom with substantial spin-orbit interaction was present in the molecules. In contrast to these gas-phase studies, electrons transmitted through organized monolayers of dipolar-chiral molecules display a large dependence on the handedness of the molecules (*6*–*8*). Several models have been presented for explaining those observations; however, they failed to provide quantitative agreement with the experimental observations (*26*, *27*).

If the effect described here is caused by a pseudo-magnetic field within the monolayer, it means that a field exceeding a few hundred Tesla must be present. Similar arguments have recently been given for the observations in strained graphene (*4*). Hence, this study identifies the need to revise our understanding of the interaction of electrons and their spin with chiral organic monolayers. The electrons that are filtered out by the layer are captured by the DNA and tunnel back to the grounded substrate. The present study indicates that the capturing of low-energy electrons by DNA is highly spin selective. The role of spin in electron-biomolecule interactions has usually been ignored. Our results indicate that the spin may play an important role in electron-DNA interactions in biological systems and open new possibilities for explaining the origin of enantioselectivity in nature. Finally, based on the phenomenon observed, it is possible to apply self-assembled monolayers of chiral molecules as very efficient spin filters at room temperature for spintronic applications (*28*–*30*).

References and Notes

1. A. Brinkman *et al.*, *Nat. Mater.* **6**, 493 (2007).
2. X.-L. Qi, S.-C. Zhang, *Phys. Today* **63**, 33 (2010).
3. Y.-W. Son, M. L. Cohen, S. G. Louie, *Nature* **444**, 347 (2006).
4. N. Levy *et al.*, *Science* **329**, 544 (2010).
5. J. Brede *et al.*, *Phys. Rev. Lett.* **105**, 047204 (2010).
6. K. Ray, S. P. Ananthavel, D. H. Waldeck, R. Naaman, *Science* **283**, 814 (1999).
7. R. Naaman, Z. Vager, *MRS Bull.* **35**, 429 (2010).
8. S. G. Ray, S. S. Daube, G. Leitus, Z. Vager, R. Naaman, *Phys. Rev. Lett.* **96**, 036101 (2006).
9. We chose to investigate in this study longer DNA because of its improved stability, as double helix, as compared to the shorter oligomers studied in (*8*).
10. T. Aqua, R. Naaman, S. S. Daube, *Langmuir* **19**, 10573 (2003).
11. H. Ron, S. Matlis, I. Rubinstein, *Langmuir* **14**, 1116 (1998).
12. T. Z. Markus *et al.*, *J. Am. Chem. Soc.* **131**, 89 (2009).
13. N. F. Mott, *Proc. R. Soc. A* **124**, 425 (1929).
14. N. F. Mott, *Proc. R. Soc. A* **135**, 429 (1932).
15. A. Gellrich, J. Kessler, *Phys. Rev. A* **43**, 204 (1991).
16. D. Oberli, R. Burgermeister, S. Riesen, W. Weber, H. C. Siegmann, *Phys. Rev. Lett.* **81**, 4228 (1998).

17. Y. Lassailly, H. Drouhin, A. van der Sluijs, G. Lampel, C. Marliere, *Phys. Rev. B* **50**, 13054 (1994).
18. D. P. Pappas *et al.*, *Phys. Rev. Lett.* **66**, 504 (1991).
19. C. Gröbli, D. Guarisco, S. Frank, F. Meier, *Phys. Rev. B* **51**, 2945 (1995).
20. M. Getzlaff, J. Bansmann, G. Schönhense, *Solid State Commun.* **87**, 467 (1993).
21. C. Cacho, Y. Lassailly, H.-J. Drouhin, G. Lampel, J. Peretti, *Phys. Rev. Lett.* **88**, 066601 (2002).
22. G. Schönhense, H. C. Siegmann, *Ann. Phys. (Leipzig)* **2**, 465 (1993).
23. H. J. Drouhin, *Phys. Rev. B* **56**, 14886 (1997).
24. T. Maruyama *et al.*, *Phys. Rev. Lett.* **66**, 2376 (1991).
25. S. Mayer, J. Kessler, *Phys. Rev. Lett.* **74**, 4803 (1995).
26. S. S. Skourtis, D. N. Beratan, R. Naaman, A. Nitzan, D. H. Waldeck, *Phys. Rev. Lett.* **101**, 238103 (2008).
27. S. Yeganeh, M. A. Ratner, E. Medina, V. Mujica, *J. Chem. Phys.* **131**, 014707 (2009).
28. G. A. Prinz, *Science* **282**, 1660 (1998).
29. S. A. Wolf *et al.*, *Science* **294**, 1488 (2001).
30. D. D. Awschalom, M. E. Flatté, *Nat. Phys.* **3**, 153 (2007).

31. T.Z.M. and R.N. acknowledge the partial support from the Israel Science Foundation.

Supporting Online Material

www.sciencemag.org/cgi/content/full/331/6019/894/DC1
Materials and Methods
Figs. S1 to S8
References

20 October 2010; accepted 20 December 2010
10.1126/science.1199339

Capillary Forces in Suspension Rheology

Erin Koos* and Norbert Willenbacher

The rheology of suspensions (solid particles dispersed in a fluid) is controlled primarily through the volume fraction of solids. We show that the addition of small amounts of a secondary fluid, immiscible with the continuous phase of the suspension, causes agglomeration due to capillary forces and creates particle networks, dramatically altering the bulk rheological behavior from predominantly viscous or weakly elastic to highly elastic or gel-like. This universal phenomenon is observed for a rich variety of particle/liquid systems, independent of whether the second liquid wets the particles better or worse than the primary liquid. These admixtures form stable suspensions where settling would otherwise occur and may serve as a precursor for microporous polymer foams, or lightweight ceramics.

The rheology and flow of suspensions is usually controlled by the interplay between the attractive van der Waals forces, repulsive electrostatic forces, or steric interactions among particles hydrodynamic interactions and Brownian forces (*1*–*6*). Capillary forces, which play a dominant role in wet granular materials, can also be an important factor in suspensions. In granular media, the addition of water, either directly or due to aging in a humid environment (*7*, *8*), is associated with an increase in the angle of repose and grain cohesiveness (*9*–*11*). The water wets the grains, creating a network of grains connected by pendular bridges, and allows, for example, the creation of complex structures such as sandcastles (*12*, *13*). In suspensions, this behavior can be reproduced through the addition of small amounts of a second immiscible fluid that preferentially wets the solid particles (*14*–*16*) and creates pendular bridges between particles causing the agglomeration of individual particles and, if the volume fraction of solids is sufficient, creates a network of particles within the bulk fluid. The addition of this secondary "binder" fluid will cause an increase in sedimentation volume (*17*–*19*), indicating network formation within the suspension. This agglomeration of particles has been used to separate solids from bulk fluid (*20*) in coal and ore preparation (*21*, *22*), to separate oil sands, and for dye-pigment preparation (*23*). This state, in which the secondary fluid preferentially wets the particles, is termed the "pendular" state because of the pendular bridges formed between particles. This state is analogous to the pendular state in wet granular media in which the fluid saturation is small and is primarily responsible for the granulation of powders (*24*, *25*).

In addition to particle agglomeration caused by the addition of a binder fluid in the pendular state, one can imagine a situation where the second immiscible fluid does not preferentially wet the particles. In this state, though the second fluid is attached to the particles and agglomeration still occurs, there is no pendular bridge formed between the particles. The addition of the secondary fluid is able to agglomerate the particles and create sample-spanning network structures due to the strong capillary force from the bulk wetting fluid. This state is analogous to the capillary state in wet granular media, where almost all of the pores between particles are filled with water (or another wetting fluid) (*26*, *27*). In wet granular materials, strong cohesive strength is observed slightly below complete saturation of the solids by the wetting fluid. In these suspensions, the secondary, preferentially nonwetting fluid is playing the part of the unfilled voids in wet granular materials where the saturation by the preferentially wetting fluid is high. In our analogy to wet granular materials, we term these admixtures "capillary" suspensions.

Despite how well the analogy describes the behavior—and the use of capillary forces in suspensions for solid/liquid separation for more than a century (*20*)—this phenomenon has not been considered with respect to rheology and formulation of stable suspensions at particle loadings substantially lower than dense pack-

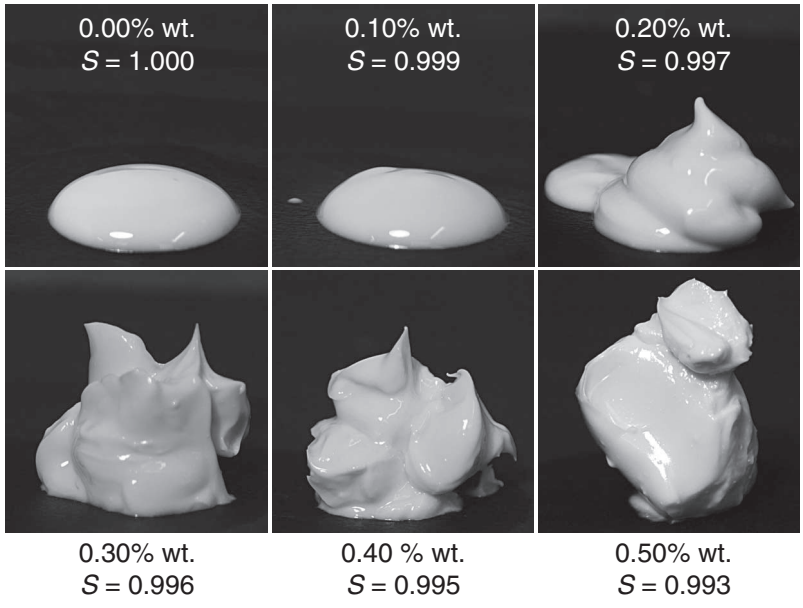

Fig. 1. The transition from weakly elastic, fluidlike behavior to highly elastic, gel-like behavior is visible with the addition of small amounts of water to a suspension of hydrophobically modified calcium carbonate (Socal, $r = 0.8$ μm, $\phi = 0.111$) in DINP. The wetting angle between the solid and water in DINP is $\theta = 139.2°$, and S is the percentage of the total liquid volume occupied by preferentially wetting fluid DINP (*31*).

Institute for Mechanical Process Engineering and Mechanics, Karlsruhe Institute of Technology, Gotthard-Franz-Straße 3, Building 50.31, 76131 Karlsruhe, Germany.

*To whom correspondence should be addressed. E-mail: erin.koos@kit.edu